Eur Biophys J (1990) 18:101–115

European Biophysics Journal

Padé-Laplace method for the analysis of time-resolved fluorescence decay curves

Ž. Bajzer*, J. C. Sharp, S. S. Sedarous, and F. G. Prendergast

Department of Biochemistry and Molecular Biology, Mayo Foundation, Rochester, MN 55905, USA

Received June 21, 1989/Accepted in revised form December 1, 1989

Abstract. The interpretation of fluorescence intensity decay times in terms of protein structure and dynamics depends on the accuracy and sensitivity of the methods used for data analysis. The are many methods available for the analysis of fluorescence decay data, but justification for choosing any one of them is unclear. In this paper we generalize the recently proposed Padé-Laplace method [45] to include deconvolution with respect to the instrument response function. In this form the method can be readily applied to the analysis of time-correlated single photon counting data. By extensive simulations we have shown that the Padé-Laplace method provides more accurate results than the standard least squares method with iterative reconvolution under the condition of closely spaced lifetimes. The application of the Padé-Laplace method to several experimental data sets yielded results consistent with those obtained by use of the least squares analysis.

Key words: Padé approximants – Fluorescence lifetime

1. Introduction

The analysis of experimental data in such diverse areas as biophysics and biochemistry, nuclear physics, electrical engineering, economics, electrophysiology, physical chemistry, medical physics and nuclear medicine frequently involves curves that are modeled as a linear combination of exponential decays:

$$f(t)=\sum_{k=1}^{n} A_k \, e^{-t/\tau_k}, \quad t\geq 0, \quad \tau_k>0, \quad A_k=f_k/\tau_k.$$

The desired information is carried by the parameters n (number of components), A_k or f_k (amplitudes or fractions) and τ_k (lifetimes or time constants). The problem of estimating these parameters from the numerically tabulated function $f(t)$, is a classic ill-conditioned problem of numerical analysis. Thus, in real situations when $f(t)$ is represented by a noisy experimental curve, the detection of the number of components and an accurate estimation of parameters can be in some circumstances, an almost insurmountable problem. This issue has been prophetically expressed in the famous book on applied analysis by Lanczos (1956). After showing an example of how one can fail in the determination of the number of components, Lanczos said: "It would be idle to hope that some other modified mathematical procedure could give better results, since the difficulty lies not with the manner of evaluation but with the extraordinary sensitivity of the exponents and amplitudes to very small changes of the data, which no amount of least-square or other form of statistics could remedy. The only remedy would be an increase of accuracy to limits which are far beyond the possibilities of our present measuring devices." (p. 279). Interestingly, the Lanczos example was recently revisited by Yeramian and Claverie (1987) and apparently they were able to determine the right number of components and were also able to estimate the other parameters rather accurately by use of a method they proposed – the so called Padé-Laplace (PL) method.

The extraction of fluorescence decay lifetimes from time-correlated single photon counting (TCPC) measurements is generally an even more difficult problem than the analysis of curves modeled by $f(t)$. The reason is that the multiexponential function is convolved with an instrument response function, (IRF) and the deconvolution is, by itself, an ill-conditioned numerical problem. A *favorable* characteristic of this problem is the possibility to control the level of noise and the ability to obtain rather dense sampling of the fluorescence intensity decay curve. Many methods of multicomponent decay curve analysis and deconvolution have been applied to this problem: *i*) The least squares method with iterative reconvolution (LS) (Grinvald and Steinberg 1974; *ii*) the method of moments (Isenberg and Dyson 1969); *iii*) the modulating functions method (Valeur and Moirez 1973); *iv*) the

* On leave of absence from Rudjer Bošković Institute, Zagreb, Croatia, Yugoslavia
Offprint requests to: F. G. Prendergast

Laplace transform method (Gafni et al. 1975); *v*) the Fourier transform method (Wild 1983); *vi*) the phase plane method (Demas and Adamson 1971; Jezequel et al. 1982); *vii*) the maximum likelihood method (Hall and Selinger 1981); *viii*) the global analysis approach (Eisenfeld and Ford 1979; Knutson et al. 1983), and most recently *ix*) the maximum entropy method (Livesey and Brochon 1987). The very fact that so many methods have been used suggests that none of them is completely satisfactory. O'Connor et al. (1979) performed a rather complete comparison of 9 techniques applied to that analysis of measured fluorescence decay curves for well characterize fluorophores. They concluded that the LS and modulating function methods appear to have the greatest ability to resolve closely spaced lifetimes but they recommended the LS method because it "can be used with no loss in accuracy to fit any chosen section of the decay curve" [1]. There are many studies in which one method is assessed or at most two methods are compared (e.g. Andre et al. 1979; Ameloot and Hendrickx 1983; Selinger and Harris 1983; Catteral and Duddell 1983; Isenberg 1983; Eisenfeld 1983; Wild 1983; Gafni 1983; Szabo and Bramall 1983; Ameloot et al. 1986; Alcala et al. 1987; Vincent et al. 1988; Small et al. 1989; Mérola et al. 1989). Most of these are limited to a small number of controlled tests by simulations, and there is an obvious lack of a unique and elaborated procedure for fair comparison between the methods. The most complete studies by simulations considered 7 different methods, and were performed by McKinnon et al. (1977), but only for two-component decays. They concluded that the LS method is marginally better in its sensitivity to noise and its ability to separate components when tested on simulated data with a rapidly decaying lamp profile, but is superior to other methods for the long tailed instrument response functions. Since present day laser technology offers a very narrow decaying IRF, there is no need to discriminate the methods on the basis of their ability to accommodate a long tailed IRF. The preference for LS is reiterated in the book of O'Connor and Phillips (1984), which may be considered as a reference book on TCPC measurements. Isenberg (1983), however, emphasizes the disadvantages of LS approach as a non-robust method. On the other hand some of the disadvantages of the LS method can be removed in the case of simultaneous analysis of several data sets in terms of the global approach (Knutson et al. 1983).

Structurally the PL method is an analytical technique which provides a *direct estimation of the number of the components* and is free of the effects of overfitting which occurs in statistical methods [2], including the maximum entropy method (Vincent et al. 1988). Recently, we have modified the Padé-Laplace method for the analysis of fluorescence intensity decays measured by multifrequency phase fluorometry (Bajzer et al. 1989 a). In this current work we have shown how the original PL method can be generalized to include a deconvolution with respect to the IRF (see also Bajzer et al. 1989 b), and we have developed a second modified version of the PL method for the analysis of time correlated single photon counting data. In addition, we performed extensive simulations to compare the standard least squares method and the PL method and then used both techniques for the analysis of experimental data for a further comparison. Our studies of two-, three-, and four-component simulated decays have suggested that *the generalized PL method (GPL) provides more accurate recovery of lifetime and fraction values than the LS method under the condition of closely spaced lifetimes*. However, in general the results from the two methods were similar. Overall, we would recommend that neither the LS method, nor the GPL method is by itself suitable for the analysis of TCPC data. A more appropriate approach might be to consider a *process* for the data analysis in which several methods of analysis might be applied in a particular sequence until a consistent set of values is obtained.

2. Experimental methods and materials

Fluorescence lifetimes were measured by time correlated single photon counting. The instrument employed is based on a mode-locked Nd:YAG laser as the excitation source. The mode-locked output was frequency doubled and used to synchronously pump a dye laser (with rhodamine 6G as the dye). The output from the dye laser was cavity dumped and then frequency doubled to yield excitation in the ultraviolet. The fluorescence was selected by use of interference or cut-off filters and detected with a Hamamatsu 1564 U-03 microchannel plate photon multiplier tube (Hedstrom et al. 1988). The time correlated photon counting was done as described in detail by O'Connor and Phillips (1984). Instrument response functions ($\approx$90 ps FWHM) for deconvolution of raw data were obtained using a scattering solution (non-dairy creamer in distilled water). Details of the data analysis procedures are given in the extended discussion below.

All of the organic chemicals were of spectrophotometric or laser grade and were used without further purification. Anthracene and POPOP were obtained from Aldrich Chemical Company. Scorpion neurotoxin variant 3 (SN-3) was the kind gift of Dr. Dean Watt (Department of Biochemistry, Creighton University) and was adjudged pure by use of electrophoretic criteria. SN-3 was used in 0.25 m*M* MOPS buffer (pH 7.0), containing 0.125 *M* KCl, with final concentration of 15 μM. Sample temperatures were maintained at 25 °C by use of Brinkmann RC3 external bath circulator connected to the sample holder.

3. Theory

The basic features of the Padé-Laplace (PL) method are described in the paper of Yeramian and Claverie (1987).

[1] This statement ignores the observation that some parts of the curve carry more information on a given component than the others. For example the tail of the curve is determined by the component with the longest lifetime and information on that component will be hidden in the first part of the curve if its corresponding amplitude is relatively small

[2] For further consideration see discussion in Sect. 5.1 below

More detailed description can be found in (Yeramian 1986; Aubard et al. 1987; Bajzer et al. 1989a). Here we derive a generalized PL method (GPL) which can be applied to the analysis of multiexponential functions convolved with a known instrument response function. Such a situation occurs in time-correlated single photon counting detection of fluorescence intensity decays.

The signal in a photon-counting experiment is the number of counts $\tilde{C}_i$ in channel i of width h:

$$\tilde{C}_i = C_i + n_i, \quad C_i = \int_{h(i-1)}^{hi} I_0(t)\,\mathrm{d}t, \quad i=1,\ldots,m. \tag{1}$$

Here n_i denotes the Poisson noise and $I_0(t)$ is the "observed" fluorescence decay function expressed as a convolution of the instrument response function $R(t)$ and the actual fluorescence intensity decay law $I(t)$:

$$I_0(t) = \int_0^t R(t-u)\,I(u)\,\mathrm{d}u = [R * I](t), \tag{2}$$

$$\tilde{R}_i = R_i + v_i, \quad R_i = \int_{h(i-1)}^{hi} R(t)\,\mathrm{d}t, \quad i=1,\ldots,m, \tag{3}$$

$$I(t) = \sum_{k=1}^{n} A_k\,\mathrm{e}^{-t/\tau_k}, \quad A_k = f_k/\tau_k, \quad \sum_{k=1}^{n} f_k = f. \tag{4}$$

$\tilde{R}_i$ is the number of counts in channel i obtained by measurement of the instrument response function; v_i is the corresponding noise (O'Connor and Phillips 1984). We assume that correction for the background is performed in usual way (cf. O'Connor and Phillips 1984, p. 158).

Now, by using the principles of the PL method (Yeramian and Claverie 1987; Bajzer et al. 1989a) we will show how the number of decay components n, lifetimes τ_k and fractions f_k can be estimated from measured quantities $\tilde{C}_i$ and $\tilde{R}_i$.

The first step is to apply the Laplace transformation to (2) and (4)

$$\hat{I}_0(p) = \int_0^\infty \mathrm{e}^{-pt} I_0(t)\,\mathrm{d}t = \hat{R}(p)\,\hat{I}(p), \tag{5}$$

$$\hat{R}(p) = \int_0^\infty \mathrm{e}^{-pt} R(t)\,\mathrm{d}t, \tag{6}$$

$$\hat{I}(p) = \int_0^\infty \mathrm{e}^{-pt} I(t)\,\mathrm{d}t = \sum_{k=1}^{n} \frac{A_k}{p+\tau_k^{-1}}. \tag{7}$$

Numerically $\hat{I}_0(p)$ can be obtained by use of the "generalized first mean value theorem of integral calculus" (Bronsthein and Semendyayev 1985) and (1):

$$\begin{aligned}\hat{I}_0(p) &= \lim_{M\to\infty} \sum_{i=1}^{M} \int_{h(i-1)}^{hi} I_0(t)\,\mathrm{e}^{-pt}\,\mathrm{d}t \\ &= \lim_{M\to\infty} \sum_{i=1}^{M} \mathrm{e}^{-\xi_i p} \int_{h(i-1)}^{hi} I_0(t)\,\mathrm{d}t = \lim_{M\to\infty} \sum_{i=1}^{M} \mathrm{e}^{-ph(i-\eta_i)}\,C_i \\ &= \sum_{i=1}^{m} \mathrm{e}^{-ph(i-0.5)}\,\tilde{C}_i + e_m(p).\end{aligned} \tag{8}$$

Here $\xi_i = hi - \eta_i h$, $0 \leqslant \eta_i \leqslant 1$. The value of η_i depends on h and $I_0(t)$, and generally is not known. In the absence of any appropriate information about the function $I_0(t)$ we choose a value of 0.5 for η_i to reduce the largest possible error. In (8) $e_m(p)$ is combined error arising from: *a*) cut-off at channel number m; *b*) noise n_i – replacement of C_i by $\tilde{C}_i$ and *c*), the choice of η_i as 0.5. The Laplace transform of the instrument response function $\hat{R}(p)$ can be numerically evaluated in a completely analogous way:

$$\hat{R}(p) = \sum_{i=1}^{m} \mathrm{e}^{-ph(i-0.5)}\,\tilde{R}_i + \varepsilon_m(p). \tag{9}$$

Combining (5)–(9) we can write

$$\hat{I}(p) = \sum_{k=1}^{n} \frac{A_k}{p+\tau_k^{-1}} = \frac{\hat{I}_0(p)}{\hat{R}(p)} = Q(p) + E_m(p), \tag{10}$$

$$Q(p) = \frac{\sum_{i=1}^{m} \mathrm{e}^{-ph(i-0.5)}\,\tilde{C}_i}{\sum_{i=1}^{m} \mathrm{e}^{-ph(i-0.5)}\,\tilde{R}_i}. \tag{11}$$

Equation (10) states that the function $Q(p)$ (which can be evaluated from the data for any p) is a rational function of p up to the error $E_m(p)$ introduced by the numerical evaluation of Laplace transforms and the noise in the data. Consequently $Q(p)$ can be well represented by paradiagonal Padé approximants (Baker 1965):

$$Q(p) + E_m(p) = [N-1/N]\,Q(q) + O(q^{2N}), \quad q = p - p_0, \tag{12}$$

$$[N-1/N]\,Q(q) = A_{N-1}(q)/B_N(q), \quad N=1,2,\ldots, \tag{13}$$

$$\begin{aligned}A_l(x) &= a_0 + a_1 x + \ldots + a_l x^l, \\ B(x) &= 1 + b_1 x + \ldots + b_l x^l.\end{aligned} \tag{14}$$

The coefficients a_j and b_j can be algebraically constructed (Longman 1971) from Taylor-expansion coefficients of $Q(p)$:

$$d_j = \frac{1}{j!}\frac{d^j}{dp^j} Q(p)|_{p=p_0}. \tag{15}$$

The numerical evaluation of these coefficients is not as simple as in the case of the original PL method (Bajzer et al. 1989a) where $Q(p)$ is essentially given by the nominator of (11) which implies simple expression for the j-th derivative. The denominator of (11) is a consequence of the fact that the multiexponential function $I(t)$ is convolved with the instrument response function $R(t)$. In the Appendix we present an algorithm for iterative numerical evaluation of Taylor coefficients d_j.

At this point the standard procedure of the PL method can be invoked (Aubard et al. 1987; Bajzer et al. 1989a). Namely, since $Q(p)$ is represented (within the error $E_m(p)$) by the rational function $\hat{I}(p)$, paradiagonal Padé approximant $[n-1/n]\,Q(q)$ coincides with $\hat{I}(p)$ within the error introduced by the numerical procedures and by the noise in the data:

$$\sum_{k=1}^{n} \frac{A_k}{p+\tau_k^{-1}} = [n-1/n]\,Q(q) + E_m(p) + O(q^{2n}) \tag{16}$$

For $E_m(p) \equiv 0$, $O(q^{2n})$ is identically zero and the roots of $1 + b_1 q + \ldots + b_n q^n$ correspond to $-\tau_k^{-1} - p_0$. Furthermore for $N \geq n$ (and $E_m(p) \equiv 0$), $[N-1/N]\,Q(q)$ reduces to

$[n-1/n]\,Q(q)$ by cancellation of common factors (Aubard et al. 1987; Bajzer et al. 1989 a). This leads to the following algorithm for determination of n, τ_k and f_k:

1. Calculate q_k^N = Real k-th pole of $[N-1/N]\,Q(q)$, $k=1, 2, \ldots; N=1, 2, \ldots$ (q_k^N are real roots of the polynomial $1+b_1 q+\ldots+b_n q^n$ which can be found numerically);
2. Calculate residues A_k^N of $[N-1/N]\,Q(q)$ at q_k^N;

$$A_k^N=\sum_{i=1}^{N} a_{i-1}(q_k^N)^{i-1}\left[\prod_{j=1, j\neq k}^{N} b_N(q_k^N-q_j^N)\right]^{-1} \tag{17}$$

3. If the set of poles $\{q_1^N, \ldots, q_n^N\}$ and associated residues $\{A_1^N, \ldots, A_n^N\}$ appear in several consecutive Padé approximants of the order $N\geq n$, $N+1$, $N+2, \ldots, N'$ with noticeable stability, then n is the number of components in the multiexponential function. The stability is characterized by $|q_k^N-q_k^{N+1}|/|q_k^N|<\varepsilon$, $|A_k^N-A_k^{N+1}|/|A_k^N|<\varepsilon$, where ε is a prescribed tolerance. Other "spurious" $N-n$, $N-n+1$, $N-n+2, \ldots, N'-n$ poles and residues are not stable.
4. Lifetimes and fractions are given by

$$\tau_k=-(q_k^N+p_0)^{-1}, \quad f_k=A_k^N\tau_k, \quad k=1, \ldots, n. \tag{18}$$

In the next section we shall illustrate this procedure on simulated data and introduce refinements and modifications based on empirical insights.

To conclude this section we briefly comment on two more topics relevant to the fluorescence data analysis. First, the GPL method can be easily adapted for application in the reference convolution technique (Gauduchon and Wahl 1978; Wijnaendts van Resandt et al. 1982; Libertini and Small 1984; Zuker et al. 1985; Boens et al. 1988). If the reference compound decays with single-exponential kinetics $I_r(t)=\alpha\,\mathrm{e}^{-t/\tau_r}$, it can be shown (Wijnaendts van Resandt et al. 1982, Boens et al. 1988) that fluorescence intensity $I(t)$ is modeled as

$$I(t)=A\,\delta(t)+\alpha^{-1}\sum_{k=1}^{n} A_k(\tau_r^{-1}-\tau_k^{-1})\,\mathrm{e}^{-t/\tau_k},$$
$$A=\sum_{k=1}^{n} A_k/\alpha. \tag{19}$$

Laplace transform of $I(t)$ then takes the form:

$$\hat{I}(p)=A+\sum_{k=1}^{n}\frac{\beta_k}{p+\tau_k^{-1}}, \quad \beta_k=\alpha^{-1}A_k(\tau_r^{-1}-\tau_k^{-1}). \tag{20}$$

This form implies that instead of paradiagonal, diagonal Padé approximants have to be used:

$$\hat{I}(p)=Q(p)+E_m(p)=[N/N]\,Q(q)+O(q^{2N+1}). \tag{21}$$

$$[N/N]\,Q(q)=A_N(q)/B_N(q)=a_N/b_N+P_{N-1}(q)/B_N(q) \tag{22}$$

where $P_{N-1}(q)=c_0+c_1 q+\ldots c_{N-1}q^{N-1}$, $c_i=a_i-b_i\,a_N/b_N$. (Compare to (12), (13) and (14)!). The lifetimes and the constants β_k then can be obtained by an algorithm analogous to that described above (steps 1. to 4.). The values of A_k are given by α, τ_r, τ_k and β_k, and $A=a_N/b_N$. The construction of diagonal Padé approximants is again based on Taylor coefficients (15) and can be performed using Longman's algorithm (Longman 1971). Thus the GPL method can be easily applied to the analysis of data obtained by the reference convolution technique.

A second interesting topic is the analysis of multiple fluorescence intensity decay data using the global approach (Eisenfeld and Ford 1979; Knutson et al. 1983; Ameloot et a. 1986; Boens et al. 1989). We will briefly speculate how the GPL method may find its place in the global approach. The most obvious case is when one can assume that the lifetimes $\tau=(\tau_1, \ldots, \tau_n)$ do not change their values in different experiments and when amplitudes (pre-exponential factors) $A=(A_1, \ldots, A_n)$ may change arbitrarily (e.g. the mixture of monoexponentially decaying fluorophores with differing emission spectra). The Padé-Laplace method can be considered as linear mapping $\mathscr{P}$ with respect to amplitudes: $\mathscr{P}(I_0)=\{A, \tau\}$, where I_0 is the "observed" fluorescence intensity decay curve. If, say, two such curves I_1 and I_2 correspond to the same τ, this τ can be recovered by applying GPL to their linear combination: $\mathscr{P}(\gamma_1 I_1+\gamma_2 I_2)=\{\gamma_1 A_1+\gamma_2 A_2, \tau\}$, which for an appropriate choice of γ_1 and γ_2 may imply the reduction of the effects of noise. Amplitudes A_1 and A_2 can be recovered by applying $\mathscr{P}$ to $2n$ different linear combinations of I_1 and I_2 and then solving the resulting linear system of equations for A_1 and A_2. The question appears whether such scheme is effective in obtaining more accurate recoveries, than if the GPL method would be applied to any of fluorescence intensity decay curves separately. Obviously this question deserves a separate study.

4. Illustration and further development of the method

To illustrate the method, we have simulated a two-component decay with lifetimes and fractions: $\tau_1=1$ ns, $\tau_2=4$ ns, $f_1=f_2=0.5$. This two-exponential function is convolved with a measured instrument response function (peak value: 40 000 counts, channel width: 0.025 ns/channel, 512 channels) and Poisson noise is added (a noise generator from Press et al. 1986 was used). The obtained fluorescence decay function is then analyzed by use of the GPL method described in the previous section. The results are shown in Table 1 where the lifetimes (τ_i^R) and fractions (f_i^R), obtained from 9 consecutive paradiagonal Padé approximants are displayed (second and third column). For brevity, the recovered lifetimes and fractions corresponding to a Padé aproximant $[N-1/N]$ we shall call "the recovery N", It is clear that recoveries 6 and 7 are relatively the most stable, i.e. the values of corresponding lifetimes and fractions are within 0.05%.

A closer look to the poles of consecutive Padé approximants of the order of 4 or more is provided by Table 2. The poles for a given N are ordered according to descending related amplitudes. Two first poles are rather stable appearing for all N (except $N=8$) and their amplitudes are larger than those corresponding to other poles. Furthermore most of the other poles lead either to negative or to complex lifetimes, so they have to be excluded a priori. The third pole for $N=5$ correspond to a very small fraction of 0.0006 and can be discarded if the fraction values is limited from below (0.01 is a reasonable limit which we will assume, if not otherwise stated). In this way we are left with 4 additional spurious poles: 1 and 2 for

$N=8$ and the poles 3 for $N=9$ and $N=3$ (see also Table 1).

In the fourth column of Table 1 we display the quantity:

$$D=[Q(0)-\sum_{k=1}^{r}\tilde{f}_k]/Q(0), \tag{23}$$

where r is the number of recovered components, $\tilde{f}_k$ are non-normalized recovered fractions and $Q(0)$ is given by (11). Note that the recovered fractions displayed in Table 1 are normalized to unity. To show the meaning of D we consider the equalities

$$\hat{I}(0)=\int_0^\infty I(t)\,dt=\sum_{k=1}^{n} f_k=f=\frac{\hat{I}_0(0)}{\hat{R}(0)}=Q(0)+E_m(0), \tag{24}$$

Table 1. Recoveries by consecutive Padé approximants

N	τ_i^R	f_i^R	D	χ^2	S	E
1	1.3401	1.0000	$1.6\cdot10^{-1}$	663.486	1.2910	0.8350
2	3.5464	0.5296				
	0.9631	0.4704	$-1.3\cdot10^{-2}$	6.674	1.2910	0.0672
3	4.4701	0.4607				
	1.1070	0.4954				
	0.6247	0.0439	$-4.1\cdot10^{-2}$	2.452	1.0942	0.5781
4	3.9456	0.5039				
	0.9944	0.4961	$-2.8\cdot10^{-2}$	0.925	1.0540	0.0087
5	4.0698	0.4959				
	1.0074	0.5041	$-3.2\cdot10^{-2}$	0.971	0.0190	0.0103
6	3.9226	0.5015				
	0.9983	0.4985	$-2.6\cdot10^{-2}$	1.173	0.0171	0.0068
7	3.9236	0.5015				
	0.9984	0.4985	$-2.6\cdot10^{-2}$	1.166	0.0001	0.0067
8	1.8895	0.7980				
	0.8159	0.2020	$-1.2\cdot10^{-1}$	461.884	0.6010	0.5663
9	4.2904	0.4227				
	1.0891	0.5565				
	0.5521	0.0208	$-6.1\cdot10^{-3}$	18.803	1.0764	0.6073

which follow from (4), (5) and (10). It follows that

$$D=[Q(0)-f-\varepsilon_{rn}]/Q(0)=-[E_m(0)+\varepsilon_{rn}]/Q(0),$$

$$\varepsilon_{rn}=\sum_{k=1}^{r}\tilde{f}_k-\sum_{k=1}^{n}f_k. \tag{25}$$

Thus the quantity D measures the error $E_m(0)$ introduced by cut-off and noise in the data and the error ε_{rn} in the recovery of the sum of fractions. $|D|$ should be much smaller than any individual normalized recovered fraction $f_k^R=\tilde{f}_k/\sum_{k=1}^{r}\tilde{f}_k$. If this is not the case we have an indication that the equalities (24) do not hold (which means that assumed multiexponential model is not adequate), and/or that the recovered fractions deviate considerably from the true values (see for example recovery 8 of Table 1).

The standard measure of the quality of the recovered parameters and the adequacy of the model is the reduced χ^2 which is defined as:

$$\chi^2=\frac{1}{m-2r}\sum_{i=1}^{m}\frac{[\tilde{C}_i-C_i^R]^2}{\tilde{C}_i} \tag{26}$$

where C_i^R is the number of counts as given by recovered lifetimes τ_k^R and the corresponding amplitudes, A_{kR}:

$$C_i^R=\int_{h(i-1)}^{hi}dt\int_0^t R(u)\,I^R(t-u)\,du=\sum_{k=1}^{r}A_{kR}\,G_i(\tau_k^R), \tag{27}$$

$$I^R(t)=\sum_{k=1}^{r}A_{kR}\,e^{-t/\tau_k^R},$$

$$G_i(\tau_k^R)=h\left[\sum_{j=1}^{i-1}e^{h(i-j)/\tau_k^R}\,\tilde{R}_j+\tilde{R}_i/2\right]+O(h^2/\tau_k^R). \tag{28}$$

(Discretized expression (27) was also used to generate the synthetic fluorescence intensity decay data.) As can be seen from Table 1, χ^2 (column 4) is reasonably close to 1 for recoveries 4, 5, 6, and 7. These are the "best" recoveries in the sense that recovered lifetimes τ_k^R and fractions f_k^R are closest to the true values τ_k and $f_k'=f_k/\sum_{k=1}^{n}f_k$ respec-

Table 2. Poles of consecutive Padé approximants

N	Pole 1	Pole 2	Pole 3	Pole 4	Pole 5	Pole 6	Pole 7	Pole 8	Pole 9
4[a]	−1.006	−0.253	2.153	2.153					
	0	0	3.356	−3.356					
5	−0.993	−0.246	−30.31	4.912	0.528				
	0	0	0	0	0				
6	−1.002	−0.255	20.13	6.051	0.363	0.363			
	0	0	0	0	0.389	−0.389			
7	−1.002	−0.255	20.24	6.046	0.365	0.363	1.317		
	0	0	0	0	0.389	−0.389	$<10^{-8}$		
8	−0.529	−1.226	−0.281	−0.281	6.972	6.972	0.108	0.108	
	0	0	0.324	−0.324	1.850	−1.850	0.877	−0.877	
9	−0.918	−0.233	−1.811	−0.025	−0.025	6.880	6.880	0.189	0.189
	0	0	0	0.295	−0.295	1.880	−1.880	0.904	−0.904

[a] For a given N, $\mathrm{Re}(q_k^N)+p_0$ is shown in the first row, and $\mathrm{Im}(q_k^N)$ is shown in the second row

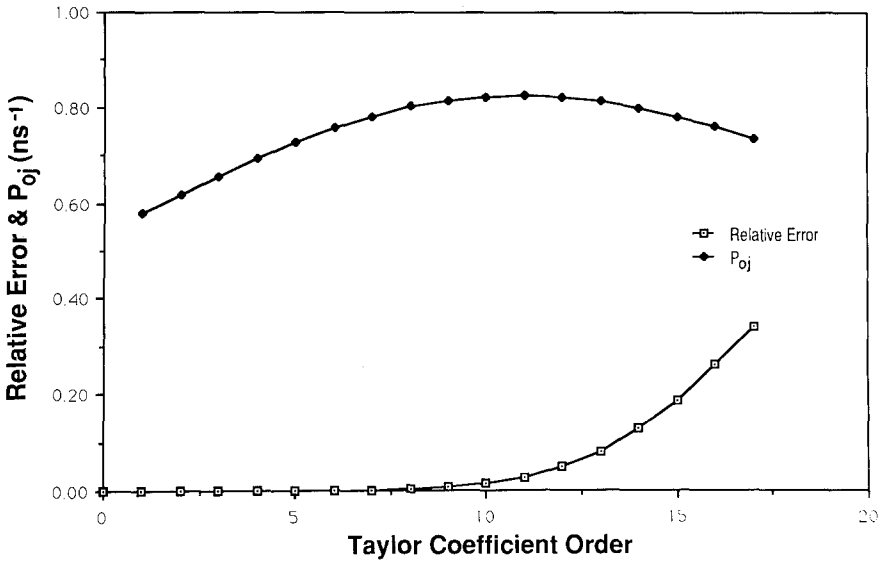

Fig. 1. Relative error in the calculation of Taylor coefficients as given by $|d_j^{\text{calc}}/d_j^{\text{exact}}-1|$, $j=1,\ldots,17$, and p_{0j} as given by (31) for the illustrative example of Sect. 2. For $j=1,\ldots,8$, the relative error ranges from 0.0002 to 0.0027

tively. In simulations where these values are known, we measure this deviation by the average relative error E displayed in the last column of Table 1. To take also into account the possible difference in the number of recovered components r and true number of components n, E is defined as:

$$E=\frac{1}{2n}\left[2|r-n|+\sum_{k=1}^{\mu}\left(\left|\frac{\tau_k-\tau_j^R}{\tau_k}\right|+\left|\frac{f_k'-f_j^R}{f_k'}\right|\right)\right], \qquad (29)$$

$$\mu=\min(n, r).$$

where j is such that for given k, $|\tau_k-\tau_j^R|$ is minimal. In other words, those recovered lifetimes are taken into account which are closest to the true values, and a penalty of $1/n$ is given when the recovery has one component more or less than the true number of components. We found the average relative error to be very useful in assessing the PL and least-square methods by simulations.

As we pointed out in the previous section, the PL method seeks those recoveries which appear in consecutive Padé approximants with noticeable stability. In Table 1 these are the recoveries 4, 5, 6 and 7. The relative stability (6th column of Table 1) of two recoveries corresponding to the orders N_1 and N_2 is measured by the function similar to E but more symmetrical:

$$S(N_1, N_2)=|r(N_1)-r(N_2)|+\frac{1}{2\mu'}\sum_{k=1}^{\mu}[F(\tau_k(N_1), \tau_j(N_2))+F(f_k(N_1), f_j(N_2))],$$

$$F(x, y)=|x-y|/y+|x-y|/x. \qquad (30)$$

Here $\tau_k(N), f_k(N)$, $k=1,\ldots,r(N)$ represent the recovery corresponding to the order N of Padé approximants, $\mu=\min[r(N_1), r(N_2)]$, $\mu'=\max[r(N_1), r(N_2)]$, and j is such that for a given k, $|\tau_k(N_1)-\tau_j(N_2)|$ is minimal. The smaller is the value of $S(N_1, N_2)$ the two recoveries corresponding to N_1 and N_2 are relatively more stable. In Table 1, column 6 we displayed $S(N-1, N)$ for $N=1, 2, 3, 4$ where by definition $S(0, 1)=S(1, 2)$. We found empirically that it is more convenient to measure relative stability of higher order Padé approximants calculating $S(N', N'')$, $N''=5,\ldots$, where $N'<N''$ corresponds to the previous recovery with minimal S. This lets our measure of stability take account of the loss of accuracy in calculation of the Taylor coefficients (see Fig. 1).

From the above discussions it might seem most reasonable to choose the most stable recovery (minimal S) as the final outcome of a GPL analysis. However we found empirically that it is useful to take also the minimal χ^2 into account. To do so we established the following procedure: The recoveries were ranked according to S and according to χ^2; the recovery withe the minimal sum of these two ranks is the chosen final outcome of our GPL method. In the example shown in Table 1 this is recovery 7, which is also the "best" recovery with respect to the average relative error E. Note that recovery 7 is not the one with the minimal χ^2.

The only free parameter of the PL method is p_0. Theoretically, the PL method should work for any p_0, for which the Laplace transform converges. However, numerical experiments have shown that the optimal $p_0(p_{0,op})$ can be estimated from the following limit (Yeramian 1986):

$$p_{0,op}=\lim_{j\to\infty} p_{0j},\ p_{0j}=p_{0,in}+1+d_j/d_{j+1}, \qquad (31)$$

where d_j are given by (15) and $p_{0,in}$ is an initial value of p_0. The sequence p_{0j} for our example is shown in Fig. 1. The limiting value is not so evident (as it is in case of noiseless data), but we can estimate it satisfactorily by taking $p_{0,op}=p_{0j}$, where j is such that $(p_{0j-1}+p_{0j+1})/2$ is minimal (the smallest slope). Such a value of $p_{0,op}$ is noticeably self-consistent, i.e. if a given value for $p_{0,op}$ is used as $p_{0,in}$ in formula (31) the newly obtained value for $p_{0,op}$ is close to the previous one. Thus, in the considered example, we started with $p_{0,in}=1\,\text{ns}^{-1}$ and obtained recursively $p_{0,op}=0.8297, 0.8250, 0.8248\ \text{ns}^{-1}$. The procedure for obtaining $p_{0,op}$ can be then summarized as follows:

1. Choose $p_{0,in}$ (we have chosen $1\,\text{ns}^{-1}$.) and set $I_{\text{old}}=0$.
2. Calculate p_{0j} for $j=0, 1,\ldots, 2N-1$, according to (31) and set $I=I_{\text{old}}+1$.

3. Find $p_{0,op}(I)=\min_{j=1,\ldots,2N-1}[(p_{0j-1}+p_{0j+1})/2]$

4. If $I\geq 2$ and $|p_{0,op}(I)-p_{0,op}(I-1)|<$tolerance (usually we used 0.03 ns^{-1}), then $p_{0,op}=p_{0,op}(I)$. Otherwise, set $I_{old}=I$, $p_{0,in}=p_{0,op}(I)$ and go to step 2.

The original PL method did not include a procedure to estimate the uncertainties of recovered parameters. In a recent application of the PL method to multifrequency phase/modulation data (Bajzer et al. 1989 a) we proposed a procedure based on variations in the p_0 parameter. The recovered parameters for varying values of p_0 will differ, owing to the influence of noise and inaccuracies introduced by the numerical procedures. By evaluating the parameters for a sample of p_0 values around $p_{0,op}$ we can estimate the errors in the recovered parameters. Let τ_{ki} and f_{ki} be the recovered lifetimes and fractions respectively, obtained for $p_0=p_i$ as described above (the recovery with minimal rank with respect to χ^2 and stability), and let

$$p_i=p_{0,op}+g_i\sigma, \quad i=1,\ldots,L, \tag{32}$$

where g_i is the random variable normally distributed and σ is the chosen standard deviation. The final estimate of the lifetimes, fractions and corresponding uncertainties is the given by

$$\bar{\tau}_k = \frac{1}{L}\sum_{i=1}^{L}\tau_{ki}, \quad \sigma(\tau_k)=c\left[\sum_{i=1}^{L}(\bar{\tau}_k-\tau_{ki})^2/L\right]^{1/2} \tag{33}$$

$$\bar{f}_k = \frac{1}{L}\sum_{i=1}^{L} f_{ki}\Big/\sum_{l=1}^{r} f_{li},$$

$$\sigma(f_k)=c\left[\sum_{i=1}^{L}\left(\bar{f}_k-f_{ki}\Big/\sum_{l=1}^{r} f_{li}\right)^2/L\right]^{1/2}. \tag{34}$$

The number c is chosen to be $\sqrt{3}$, which according to the Chebyshev inequality (see, for example, Kempthorne and Folks 1971) means that at least 2/3 of the population deviate from the population mean by σ or less. This inequality holds for an arbitrary distribution. In the example considered for $L=32$, $p_{0,o}=0.825$ ns^{-1} and $\sigma=0.03$ ns^{-1}, we obtained: $\bar{\tau}_1=(3.96\pm0.08)$ ns, $\bar{\tau}_2=(1.000\pm0.005)$ ns, $\bar{f}_1=0.500\pm0.003$, $\bar{f}_2=0.500\pm0.003$. (The results for $L=64$ were equal within uncertainties). The corresponding average relative error is: $E=0.0028$. This is smaller than the smallest average relative error obtained when the calculation is performed only for $p_{0,op}$ (see Table 1). We found this to be true in 62% cases of 431 simulations, with various lifetimes and fractions.

The procedure established in this secton for estimating the number of components, lifetimes and fractions will be now used in simulations studies and for analysis of real data.

5. Results and discussion

5.1 Simulations

The original PL method has been tested on simulated exponentially decaying events with excellent results (e.g. Table 5 of Aubard et al. 1987 and Table 1 of Matheson 1989 show comparison with other methods for multiexponential analysis; see also Yeramian and Claverie 1987; Yeramian 1986). In continuation of our preliminary work (Bajzer et al. 1989 b) here we tested the generalized Padé-Laplace method for analysis of time-resolved fluorescence decay measurements.

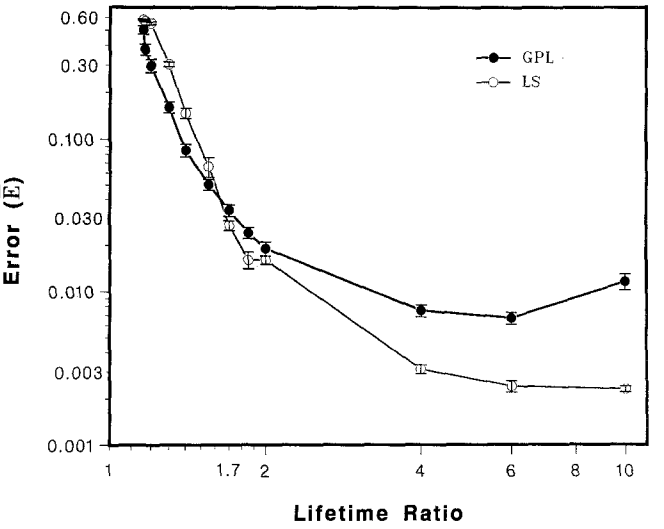

Fig. 2. The average relative error (with one standard deviation) in recovered lifetimes and fractions for 64 samples of noise as a function of lifetime ratio for two-component simulations. The fractions were equal and $\tau_1=1$ ns. The results for the LS(○) and GPL (●) method are shown. The simulations were based on measured instrument response function comprising 512 data points, 40 000 counts at peak and channel width of 0.025 ns/channel, FWHM $\approx$ 0.09 ns^{-1}. The peak value of simulated fluorescence intensity decay profile was limited to 40 000 counts + noise

The simulations were chosen to show both the effectiveness and limits of the method. For a given level of noise in the data, determined by the number of counts per channel, the crucial limitation in recovery of components is the ratio of the lifetimes. For example, two components can still be resolved for some critical ratio $(\tau_1/\tau_2)_{crit}$; to demonstrate this we examined two component systems of 12 varying lifetime ratios. In Fig. 2 the average relative error E as given by (29) is shown. Each point corresponds to 64 simulations for a given pair of lifetimes and fractions. Each simulation reflects a different realization of the noise in the synthetic data. The error E_i, $i=1,\ldots,64$ is calculated for each of simulations ($L=32$ and $\sigma=0.03$ ns^{-1} is chosen) and its average $\bar{E}$, together with the standard error, is plotted against the lifetime ratio. For sake of comparison we plotted $\bar{E}$ for the GPL recoveries and for the recoveries given by the standard least-square (LS) method. Clearly the GPL method gives better results for ratios smaller than 1.7, while the standard method seems to be better for higher ratios. The steep decrease of $\bar{E}$ with lifetime ratio and a subsequent leveling off are otherwise characteristics of both methods. Above a ratio of 2 both methods are reasonably accurate with an average error in recovered parameters of less than 2%. The increase in $\bar{E}$ for GPL at lifetime ratio of 10.0 is caused by the 12.8 ns cut-off in simulated data which in this particular simulation leads to an incomplete evalua-

Table 3. Recovered lifetimes and fractions of selected simulations

	τ_1	τ_2	τ_3	τ_4	f_1	f_2	f_3	f_4	E
Exact	1.00	1.16			0.50	0.50			0
GPL	0.70	1.10			0.06	0.94			0.53
LS	0.54	1.09			0.01	0.99			0.60
Exact	1.00	1.17			0.50	0.50			0
GPL	0.90	1.14			0.22	0.78			0.31
LS	0.88	1.10			0.08	0.92			0.46
Exact	0.80	1.28	2.048		0.334	0.333	0.333		0
GPL	0.62	1.05	2.01		0.11	0.50	0.39		0.30
LS	0.88	1.77	1.88		0.513	0.487	$8 \cdot 10^{-4}$		0.39
Exact	0.40	0.80	1.60	3.20	0.25	0.25	0.25	0.25	0
GPL	0.28	0.55	1.44	3.18	0.08	0.34	0.32	0.26	0.27
LS	0.426	0.431	1.12	2.94	0.01	0.32	0.36	0.32	0.32
Exact	0.40	0.92	2.116	4.8668	0.25	0.25	0.25	0.25	0
GPL	0.34	0.70	1.89	4.89	0.16	0.28	0.30	0.26	0.15
LS	0.35	0.63	1.79	4.79	0.15	0.27	0.31	0.27	0.23
R.E.[a]	τ_1 (%)	τ_2 (%)	τ_3 (%)		A_1 (%)	A_2 (%)	A_3 (%)		E_{med}
GPL[b]	0.58	2.0	6.9		4.4	0.36	3.7		0.018
LS	0.40	6.4	5.1		4.9	0.27	8.6		0.027

[a] R.E. indicates that average relative error in recovered parameters with respect to their true values is caculated

[b] In 4 of 64 cases the GPL method recovered 4 components. These cases were disregarded in calculation of average relative errors in parameters for both methods, but were taken into account for the calculation of E_{med}

tion of the Laplace transform. However, by increasing the channel width from 0.025 ns to 0.060 ns the Laplace transform of fluorescence decay function can be calculated more accurately and the error $\bar{E}$ (GPL) decreased from 0.0116 ± 0.0014 (shown in Fig. 2) to 0.0024 ± 0.0001 (factor of 4.8) which is practically equal to $\bar{E}$ (LS) $= 0.0023 \pm 0.0001$ for the original channel width (shown in Fig. 2). For the increased channel width, $\bar{E}$ (LS) decreased only by a factor of 1.8. These results indicate that the accuracy of the GPL method is close to that of the LS method at higher lifetime ratios, providing that the fluorescence decay function counts are collected until the decay reaches the background level, or at least 3 times longer than the largest fluorescence lifetime.

Our 2-component simulations indicate that the critical lifetime ratio is ≈ 1.16. For this ratio two components were recovered (with smaller fraction being at least 0.01) in 58% of cases. However the accuracy of recoveries for both methods was poor[3]. The recovered lifetimes and fractions at respective medians of E_i for both methods are shown in Table 3. For an only slightly higher lifetime ratio of 1.17, the accuracy of recoveries by the GPL method were considerably improved and two components were recovered in 80% of the cases with median of $E_i = 0.31$ (see Table 3). For comparison we also show in Table 3 the recovered lifetimes and fractions by the LS method in the best case of minimal $E_i = 0.46$. The best result of the GPL method for this ratio is characterized by minimal $E_i = 0.01$.

[3] Under the circumstances of doubled number of data points and halved peak value counts (used later for the three- and four-component simulations) two components with lifetime ratio of 1.15 were recovered in 67% of cases with similarly poor accuracy

It is interesting to note that in rare degenerate cases with small lifetime ratio, reasonably good recoveries by the GPL method may correspond to unacceptably high values of χ^2. Thus for a ratio of 1.17 in 7 of 64 cases χ^2 for the GPL method ranged from 2.3 to 12.9 while corresponding relative errors E_i ranged from 0.05 to 0.4. For the same simulations χ^2 minimized by the LS method ranged from 0.9 to 1.2, while corresponding E_i were not smaller than 0.5. The most disparate example is characterized by the following values for χ^2, Durbin-Watson (DW) parameter (O'Connor and Phillips 1984) and corresponding error E: exact parameters: (χ^2, DW, E) = (1.06, 1.893, 0); GPL: (χ^2, DW, E) = (12.9, 0.148, 0.10); LS: (χ^2, DW, E) = (1.00, 1.947, 0.57), and by the weighted residuals shown in Fig. 3. Clearly there is a pronounced non-random structure in the residuals corresponding to the GPL method recovery while the residuals for LS recovery appear random. So, according to usually imposed criteria based on χ^2, Durbin-Watson parameter and the randomness of residuals LS recovery should be considered highly acceptable, while GPL recovery is highly unacceptable. The *truth is however, just the opposite,* as revealed by out absolute measure of the goodness of recovery, average relative error E. This example is important to illustrate the basic difference between the GPL and the LS methods: The GPL method estimates the parameters basically *without regard of how well the resulting curve fits the data,* whereas the LS method estimates parameters on the bases of the requirement that the corresponding curve *fits the data as closely as possible.* As we can see from the example shown this requirement may be insufficient when the lifetime ratio is small and the problem of parameter estimation apparently becomes more ill-conditioned. This can be seen clearly if we rewrite the expression (26)

for two components with close lifetimes τ^R and $\tau^R+\Delta\tau$:

$$\chi^2=\sum_{i=1}^{m} w_i[\tilde{C}_i-(A_{1R}+A_{2R})\,G_i(\tau^R)-\Delta_i]^2, \qquad (35)$$

$$w_i=[\tilde{C}_i(m-4)]^{-1},$$

$$\Delta_i=A_{2R}[G_i(\tau^R+\Delta\tau)-G_i(\tau^R)],$$

(cf. (27) and (28)). The term Δ_i may be of the order of the noise in $\tilde{C}_i$ and the minimization of χ^2 may effectively reveal only one component or two components with one of amplitudes being very small (this is exactly the case in considered example: $A_{1R}=0.05$, $A_{2R}=0.95$). In the interplay of the small term Δ_i with the noise, overfitting may have a considerable effect: χ^2 is minimized by the algorithm until it falls below the value of χ^2 for exact parameter values, thereby sometimes causing a substantial deviation of the estimated parameter values from the corresponding exact values.

Having basically understood how the LS method can fail in the case of close lifetimes the question arises: how one can understand the "paradox" that a high value of χ^2 (GPL) may correspond to relatively small E (GPL)? By considering (29) with $n=r$, we see that for a given E (say 0.1) it defines a region in three-dimensional space of τ_1^R, τ_2^R and $f_1^R\leq 1$ (f_2^R is constrained by $f_1^R+f_2^R=1$) characterized by the same average relative error of recovery. χ^2 is defined by (26)–(28) for any point of this space and for two different points from the specified region it may assume very different values (e.g. for $(\tau_1^R, \tau_2^R, f_1^R)=(0.8489, 1.1676, 0.4373)$, which is the GPL recovery in considered example, $\chi^2=12.9$, and for $\tau_1^R, \tau_2^R, f_1^R=(1, 1.17, 0.6)$, compatible with $E=0.1$, we obtained $\chi^2=1.74$). Even, if for instance f_1^R and τ_1^R were fixed at a certain values compatible with $E=0.1$, τ_2^R may assume two different values yielding two different values of χ^2. High χ^2 values usually correspond to the non-random residuals which we encountered in our example. It follows from the above example and discussion that *non-randomness of residuals does not necessarily imply very inaccurate recovery of parameters and vice versa that random residuals may correspond to very inaccurate recovery of parameters.*

Once again we emphasize that such degenerate cases are rare but still possible. Therefore, in practice when we deal with the real data and encounter close lifetimes as recovered by any of the methods, it is advisable to perform and appropriate simulation study. Then, by analyzing the errors E_i for different noise relizations we can assess which particular method is likely to give more accurate results.

For a lifetime ratio of 1.2, two components were recovered by the GPL method in 89% of the cases whereas for ratios higher or equal to 1.3 two components were recovered in 100% of the cases. Both the GPL and the LS method are similarly sensitive to the level of noise. For example when the noise was increased by using a measured instrument response function with a peak value of only 10 000 counts, $\bar{E}$(GPL) at a lifetime ratio of 1.3 increased by a factor of 1.8 and $\bar{E}$(LS) by a factor of 1.7. Thus at this ratio the GPL method is still characterized by $\bar{E}$ two times lower than $\bar{E}$(LS).

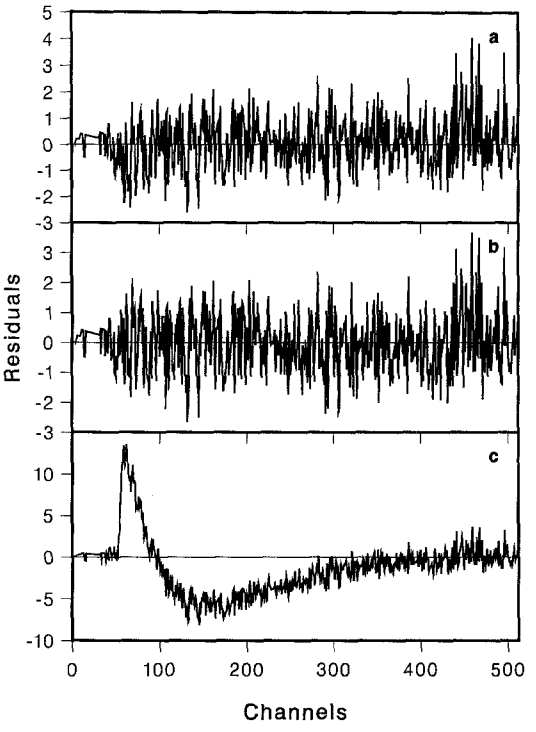

Fig. 3a–c. Residuals corresponding to the simulation with $\tau_1=1$ ns, $\tau_2=1.17$ ns, $f_1=f_2=0.5$ and the instrument response function as in Fig. 2. **a** Residuals from the exact fluorescence intensity decay curve. **b** Residuals from the LS fit. **c** Residuals from the GPL curve

We now present a more precise comparison of the results from application of GPL and LS methods on simulated date described above. To reduce the noise sample variability we computed a statistic which is the ratio E_i(GPL)/E_i(LS) of the errors of the GPL and LS methods applied to the same noise realization – 64 noise samples generate a set of 64 values of this statistic. To reduce the influence of rare outliers, we characterize this set by the median value (Fig. 4).

In Fig. 5 we show the dependence of $\bar{E}$ on fraction (normalized) of the first component. The pattern is very similar for both methods showing that the result for $f_1=f_2=0.5$ is best. For the smaller or larger ratios of fractions the recoveries are less accurate.

In Figs. 6 and 7 we show the results of three-component simulations. The successive lifetime ratios were of equal ratio, i.e. $\tau_2/\tau_1=\tau_3/\tau_2$. This ratio was varied in different simulations. When this ratio was 1.6, three components can be resolved in 64% of cases, although both methods provided rather poor recovery (Table 3 shows the recoveries at respective medians of E_i). Note that in the case of three components, according to definition of E, (29), the penalty in E for one component less, or one component more is 1/3, while it is 1/2 in the case of two components. The recovery from the LS method is practically equivalent to a two-component recovery ($E=0.39$). For a lifetime ratio 2 or higher, three components were recovered 100%. Again, as in the case of two components, the GPL method is better for smaller ratios (up to $\tau_2/\tau_1=\tau_3/\tau_2=2.3$) and the LS method is better at higher ratios.

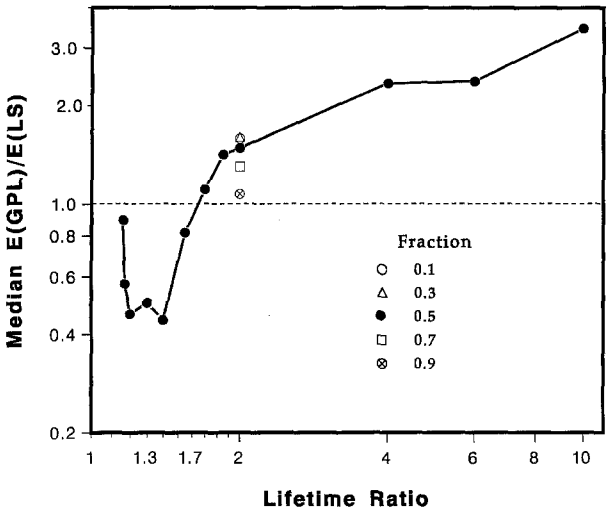

Fig. 4. Median value of statistic $E_i(\mathrm{GPL})/E_i(\mathrm{LS})$, $i=1, \ldots, 64$ as a function of lifetime ratio. E_i is given by (29); the index i denotes i-th sample of noise. Fluorescence intensity decay data are simulated as in Fig. 2 with equal and unequal fractions (the legend corresponds to the fraction f_1; $f_1+f_2=1$)

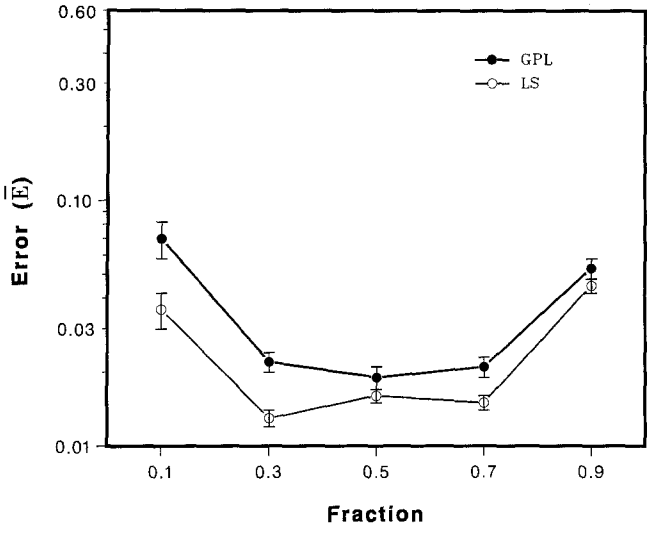

Fig. 5. The average relative error (with one standard deviation) in recovered lifetimes and fractions for 64 samples of noise as a function of fraction f_1, $(f_1+f_2=1)$ for two-component simulations. The results for the LS (o) and the GPL (•) method are shown. Fluorescence decay data were simulated as in Fig. 2

However, it is important to note that by increasing the channel width so that more information is obtained from the tail of the intensity fluorescence decay function, the results of the GPL method at higher lifetimes ratios can be improved. Thus, for example, in the case of a lifetime ratio of 3, if the channel width is doubled, $\bar{E}$ decreased from 0.029 ± 0.003 to 0.021 ± 0.002. Interestingly, the response of the LS method to doubling of channel width in this case was opposite: $\bar{E}$ increased from 0.013 ± 0.001 to 0.037 ± 0.001. One possible explanation of this behavior comes from the fact that the noise in the data is defined by a Poisson distribution and not by a Gaussian distribution

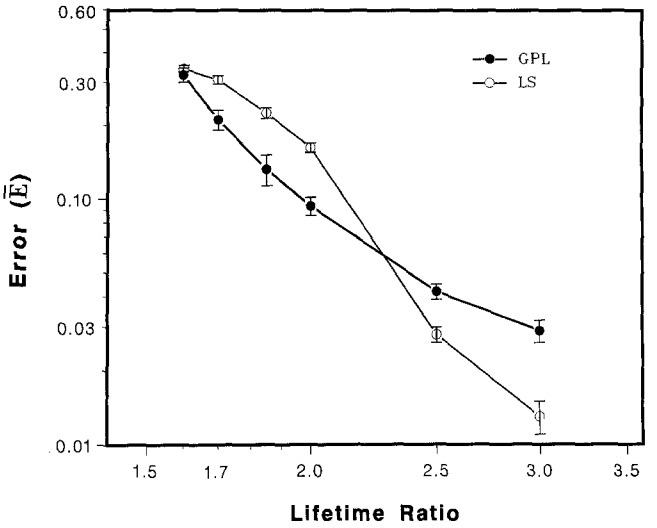

Fig. 6. The average relative error (with one standard deviation) in recovered lifetimes and fractions for 64 samples of noise as a function of lifetime ratio $\tau_2/\tau_1=\tau_3/\tau_2$ for three-component simulations. The fractions were $f_1=f_2=0.333$, $f_3=0.334$, and $\tau_1=0.8$ ns. The results for the LS (o) and GPL (•) method are shown. The simulations were based on measured instrument response function comprising 1024 data points, 21 795 counts at peak and channel width of 0.0276 ns/channel, FWHM ≈ 0.18 ns^{-1}. The peak value of simulated fluorescence decay profile was limited to 21 795 counts + noise

on which the LS method is based. A Gaussian distribution differs significantly from a Poisson distribution when there is a small number of counts (e.g. at the tail of the fluorescence decay function).

The PL method for pure multiexponential decay has been compared to other methods on the simulated 3-component example given by $\tau_1/\tau_2=\tau_2/\tau_3=5$, $A_1/A_2=50$, $A_1/A_2=250$, $A_1=25$ (Aubard et al. 1987, Table 5; Matheson 1989, Table 1). Based on this particular example and one with two components Matheson concluded "that the PL and non-linear least squares fit are significantly different, the PL fit tending to better determine the slower component of a two rate processes". In order to see whether such behavior of the PL method bears generality we simulated fluorescence intensity decay profiles for this three component example (τ_1 is scaled to 0.2 ns) with instrument response function as in Fig. 6. To obtain a statistically significant result we calculated the averages (and standard deviations) of relative errors in each of the recovered parameters based on 64 different realizations of noise. The results for the GPL and the LS method are displayed in the last two rows of Table 3, together with the values of the corresponding medians E_{med} of E_i. It is clear that both methods recovered all parameters with *similar accuracy* and that *the lifetime of the fastest component (τ_1) was the most precisely determined by both methods*. Thus the conclusion of Matheson is not generally valid.

In Figs. 7 and 8 we show the results of four-component simulations. Again, the lifetimes were chosen to have equal ratios: $\tau_2/\tau_1=\tau_3/\tau_2=\tau_4/\tau_3$, and this ratio was varied from 2 to 3. At a ratio 2 which can be considered as the critical ratio, four components were resolved in 67%

of cases, and the highest percentage of 81% was obtained for ratios of 2.3 and 2.5 (see Table 3 for representative recoveries at ratios 2 and 2.3 and at respective medians of E_i for GPL and LS). The data in Figs. 7 and 8 show that both methods give similar results. Again the GPL method somewhat dominates at lower ratios while the LS dominates at higher. However, as might be expected, both methods are less accurate in recovering the lifetimes and fractions than for the case of three components with an equal level of noise and equal number of data. We noticed that LS method is particularly sensitive to the intial guess of parameters for the four-component simulations.

The case when one of the components is characterized by a very small fraction is also of practical interest. We have therefore investigated the GPL method and compared it to the LS method on simulated data constructed for $\tau_1 = 0.4$ ns, $\tau_2 = 1$ ns, $\tau_3 = 6$ ns, $f_1 = f_2$ and f_3 assuming successively smaller values: 0.04, 0.02, 0.01, with the same impulse response function as previously used in three-component simulations. The results of this investigation summarized in Table 4 show that the GPL method [4] gives somewhat more accurae results for $f_3 = 0.04$ while the LS method is more accurate for $f_3 = 0.01$. For this smallest fraction in 17% of cases the GPL method didn't recover the small component (e.g. $\tau_3^R = 3.3 \pm 4.2$ ns, $f_3^R = 0.11 \pm 0.14$). These infrequent cases are the main reason why $\bar{E}$(GPL) is so large while the corresponding median value of E_i is practically equal to that of LS method. Based on this and other similar investigations we have done, it seems that the fraction of 0.01 is the lower limit at which the GPL method gives reasonably accurate results, although less accurate than those obtained by the LS method. These findings suggest that in cases when either of considered methods detects a component with a very small fraction, the result of LS method is likely to be more accurate.

5.2 Tests on real data

We now present examples in which we have applied the GPL method to the analysis of time-correlated single photon counting data on decay of known fluorophores and a of tryptophan bearing protein. In order to account for a possible zero-time shift in instrumental response function we have applied the version of the GPL method described in Appendix.

On first example is the fluorescence decay of POPOP in EtOH ($\approx 10\ \mu M$). The data comprised 512 data points with 10 000 counts at peak and channel width of 0.05 ns. The lifetime obtained by the GPL method (Table 5) is equal to the lifetime obtained by the LS method within the estimated uncertainty. Similar agreement is found for the lifetime of anthracene in EtOH (Table 5; 512 data points, 10 000 counts at peak, channel width: 0.05 ns). We then mixed POPOP and anthracene in such a way that count rates from each fluorophore separately were very

[4] Possible fraction values were in this case limited from below by 0.005; see Sect. 4

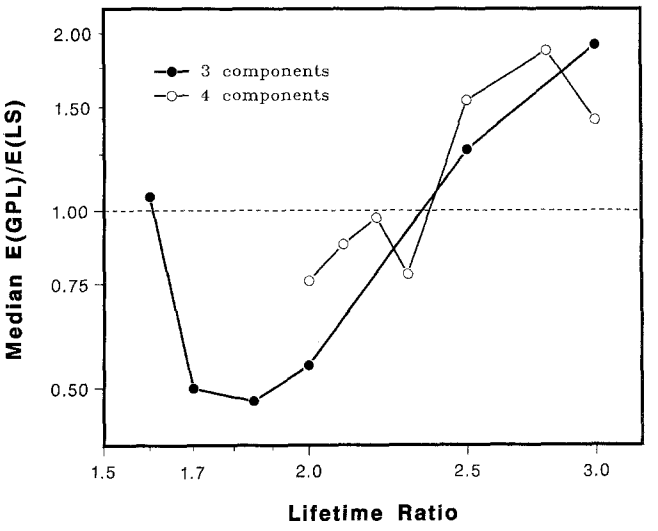

Fig. 7. Median value of statistic E_i(GPL)/E_i(LS), $i = 1, \ldots, 64$ as a function of lifetime ratio. Three-component simulations as in Fig. 6; median values denoted by (•). Four-component simulations with equal lifetimes ratio $\tau_2/\tau_1 = \tau_3/\tau_2 = \tau_4/\tau_3$, ($\tau_1 = 0.4$ ns) and equal fractions $f_1 = f_2 = f_3 = f_4 = 0.25$; median values deonoted by (o). Fluorescence decay data were simulated by use of instrument response function as in Fig. 6

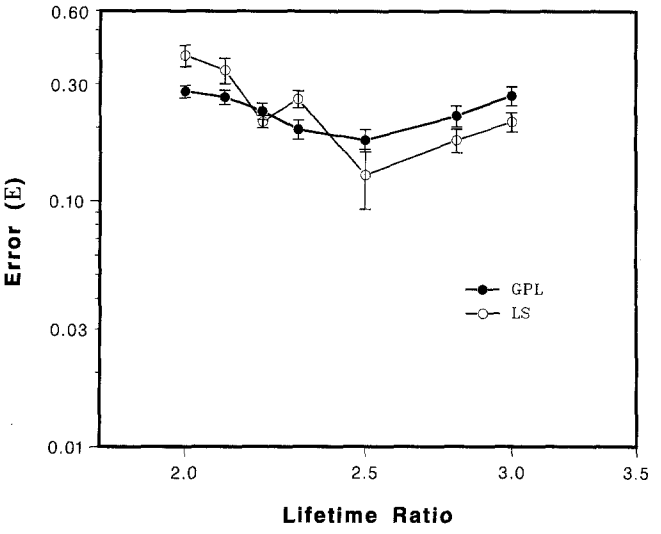

Fig. 8. The average relative error (with one standard deviation) in recovered lifetimes and fractions for 64 samples of noise as a function of lifetime ratio for four-component simulations as in Fig. 7b. The results for the LS(o) and GPL (•) methods are shown

Table 4. Accuracy of revoveries for simulations with a small third component fraction

f_3	A_1/A_2 [a]	$\bar{E}$ (LS)	E_{med} (LS) [b]	$\bar{E}$ (GPL)	E_{med} (GPL)
0.04	71.25	0.032(2) [c]	0.0287	0.023(2)	0.0168
0.02	142.5	0.029(1)	0.0242	0.030(2)	0.0265
0.01	285	0.043(1)	0.0407	0.26 (6)	0.0427

[a] The ratio of the largest and the smallest amplitude (preexponential factor)

[b] E_{med} denotes the median of E_i, $i = 1, \ldots, 64$

[c] The number in parenthesis is the estimated uncertainty in the last significant digit

Table 5. Recovered lifetimes and fractions of selected fluorophores

	τ_1	τ_2	f_1	f_2	δ	χ^2
GPL[a]	1.3279(7)[d]		1		0.0068	1.001
LS[a]	1.325 (3)		1		0.0069	0.996
GPL[b]	4.38 (1)		1		0.014	1.23
LS[b]	4.392 (5)		1		0.012	1.15
GPL[c]	1.27 (1)	4.39(3)	0.496(5)	0.504(5)	−0.024	5.78
LS[c]	1.32 (1)	4.37(3)	0.499(2)	0.501(2)	0.008	1.20

[a] POPOP
[b] Anthracene
[c] Mixture: POPOP + Anthracene
[d] The number in parenthesis is the estimated uncertainty in the last significant digit. All lifetimes and shifts δ are expressed in nanoseconds

Table 6. Recovered lifetimes and fractions of Scorpion neurotoxin

	GPL	LS(1)	LS(2)
τ_1	0.138(5)[a]	0.111 (8)	0.081 (8)
τ_2	0.48 (3)	0.48 (3)	0.39 (2)
τ_3	0.9 (2)	0.85 (5)	0.78 (2)
τ_4	4.2 (1.0)	4.72 (9)	4.71 (6)
f_1	0.089(7)	0.0888(6)	0.061 (6)
f_2	0.52 (9)	0.48 (2)	0.36 (1)
f_3	0.34 (9)	0.37 (2)	0.516 (9)
f_4	0.05 (1)	0.060 (1)	0.0608(8)
δ	−0.012	−0.015	−0.016
χ^2	1.34	1.39	1.34

[a] The number in parenthesis is the estimated uncertainty in the last significant digit; (1.0) means that the uncertainty is 1 ns. All lifetimes and shifts δ are expressed in nanoseconds

close, i.e. the fluorescence intensities observed by the PMT for each fluorophore were essentially the same, and performed the measurements under the same conditions. The recovered lifetimes are fairly consistent with the lifetimes of individual fluorophores and both the GPL and the LS methods gave practically the same result (Table 5). In order to understand the deviation of 4% in the recovery of the shorter lifetime by the GPL method from the recovered lifetime of POPOP, we performed simulations with the same instrumental response function and 64 realizations of the noise. The lifetimes, fractions and the shift of GPL recovery from Table 5 were taken as the exact values for this simulation and the GPL analysis gave: $E=0.0103$ as a median value. This indicates that the error of 4% in one parameter could be expected (note that according to definition of E if one parameter deviates from its true value for 4%, $E \geq 0.01$). The median value is in good agreement with the error $E_u=0.009$ which is calculated using (22) under the assumption that recovered lifetimes and fractions are the exact values and uncertainties obtained within GPL method (shown in parenthesis) are the deviations from the exact values. We also performed similar simulations by taking as the exact values, lifetimes, fractions and the shift of LS recovery and applying the LS method. The results gave $E=0.0104$ as a median value. This suggests that standard uncertainty estimates of the LS method (shown in parenthesis) are somewhat too low giving $E_u=0.006$. Nevertheless, the fact is that the LS method in this case gave more consistent results than the GPL method.

In Table 6 we present the results of GPL and LS analyses of fluorescence decay of the single trp residue in scorpion neurotoxin. For this protein the data comprised 512 data points with 20 000 counts at peak and channel width of 0.020 ns. GPL analysis was performed using 64 p_0 values and 4-components were recovered in 80% of cases. The LS analysis was strongly dependent on the initial guess of parameters; two different recoveries are shown in Table 6. The first is in good agreement with the recovery from the GPL method. We then simulated the data using the GPL recovery as the exact values of parameters. GPL analysis of the simulated data revealed that with this level of noise, number of data and channel width, it is more likely that only three components can be resolved. In the same time when the LS method was set for 3-component recovery, we obtained $\chi^2=1.64$ or greater, depending on initial guess of parameters. These results leads us to speculate that the multiexponential model may not be the best descriptor of the trp fluorescence of scorpion neurotoxin.

6. Conclusions

We have shown that the PL method can be generalized for use in situations where the multiexponential function is convolved with a known instrument response function. Application of this generalized PL method to the analysis of fluorescence intensity decay data obtained by time-correlated single photon counting detection is then shown to be straighforward.

We have refined the procedure for selection of the best recovery from the multiple recoveries obtained by consecutive Padé approximants. Our approach is based on combined use of a precisely defined measure of stability between two recoveries and a χ^2 value which measures how close the data are to the function given by recovered parameters. In addition we have applied and tested (by simulations) a procedure which improves the accuracy of recovered parameters and provides an estimation of corresponding uncertainties by variation of p_0 parameter (Bajzer et al. 1989a).

In order to assess the GPL method and compare it to the standard LS method we performed a great number of simulations based on measured instrument response functions. These simulations revealed:

1. The GPL method gives markedly more accurate results than the standard least-square method in the domain of closely spaced lifetimes.
2. The results of GPL method for higher lifetimes ratio were fairly accurate if the cut-off influorescence intensity decay function exceeds approximately three times the largest lifetime. However, even with the latter circumstances the results were sometimes less accurate than the results obtained by standard LS method. Similarly, when fractions as small as 0.01 are involved the LS method provided more accurate results then the GPL method.

3. The critical lifetime ratio apparently increases with the number of components present. Under the conditions of noise and number of data points we investigated, the critical lifetime ratio at which two components are still resolved was estimated by GPL method to be 1.16. For the three components this ratio was 1.6 and in case of four components it was 2.0.
4. At critical lifetime ratios which we considered the results of the GPL method and of the LS method were of comparably low accuracy.
5. For lifetime ratios somewhat above the critical, the results of the GPL method were increasingly more accurate than those of the LS method which shows a deficiency due to overfitting.
6. An increased level of noise produces similar quantitative effects on the results obtained by both methods.

Tests on experimental data gave consistent results for analysis by the GPL and the LS method. We found that in the process of data analysis it is useful to simulate fluorescence intensity data using the recovered parameters and then to apply the analysis to simulated data. In this way one can assess how adequate a given method is and how appropriate is the multiexponential model itself. The present study suggests that the GPL method is more appropriate than the standard LS method when the lifetimes are closely spaced. In addition, the GPL method intrinsically provides an estimate of the number of components, which is not based on sometimes inconclusive statistical procedures usually used with the LS method. All this suggests that in the *process* of fluorescence decay analysis, first the GPL method might be applied. Subsequently, one can apply the standard LS method with the number of components and the parameters obtained by use of GPL method as the initial guess. However, the optimal strategy for a *process* for data analysis has yet to be considered more generally as other methods should be considered as well.

A Appendix

The numerical evaluation of Taylor coefficients in (15) require the nth derivative of the quotient $Q(p)$ of the two differentiable functions whose derivatives can be calculated straightforwardly. In our application n can be as large as 35, so that a direct use of numerical differentiation algorithms might give rather inaccurate results. We propose an iterative algorithm based on Leibniz rule. Let

$$Q(p)=P(p)/R(p) \overset{\text{def}}{=} Q^{(0)}(p) \tag{36}$$

and we seek nth derivative $Q^{(n)}(p)$ when $P^{(i)}(p)$ and $R^{(i)}(p)$, $i=0,\ldots,n$ are given. According to Leibniz rule we have (p-dependence is omitted for simplicity):

$$(P/R)^{(n)}=\sum_{k=0}^{n} C_k^n\, P^{(n-k)}(1/R)^{(k)}, \tag{37}$$

where $C_k^n=n!/[n-k)!\,k!]$. $P^{(n-k)}$ is known and $(1/R)^{(k)}$ has to be determined. If the Leibniz rule is applied to equation $[R(1/R)]^{(k)}=0$ one can obtain:

$$Z_k \overset{\text{def}}{=} (1/R)^{(k)}=-(1/R)\sum_{j=1}^{k} C_j^k\, Z_{k-j}\, R^{(j)}. \tag{38}$$

Thus by using (38) we can first calculate Z_1 from $Z_0\equiv 1/R$, then Z_2 from Z_1 and Z_0, and generally Z_k from $Z_{k-1},\ldots,Z_0$. This iterative procedure can be easily implemented as a computer code.

In the follwing we treat zero-time shift δ of instrument response function (O'Connor and Phillips 1984) within the framework of GPL method. For $\delta\neq 0$ (2) becomes

$$I_o(t)=\int_0^t R(t+\delta-u)\, I(u)\, \mathrm{d}u, \quad R(x)\equiv 0, \quad x\leq 0. \tag{39}$$

By taking the Laplace transform of this equation we obtain

$$\hat{I}_o(p)=\hat{I}(p)\,\hat{R}(p)\,\mathrm{e}^{\delta p}. \tag{40}$$

The shift δ is usually of order of few channel widths and p is of the order of 1 ns^{-1}, so that δp is small compared to 1. Therefore we can expand $e^{\delta p}$ in Taylor series and generalize (10) and (12) to

$$\sum_{k=1}^{n}\frac{B_k(p)}{p+\tau_k^{-1}}+O(\delta^2 p^2)=\frac{\hat{I}_o(p)}{\hat{R}(p)}=Q(p)+E_m(p), \tag{41}$$

$$B_k(p)=(1+\delta p)\,A_k, \tag{42}$$

$$Q(p)+E_m(p)=[N/N]\,Q(p)+O(q^{2N+1}). \tag{43}$$

This implies that instead of paradiagonal, diagonal Padé approximants have to be used to obtain n, τ_k and $B_k(-1/\tau_k)$ by procedure described in Sect. 2. From (42) it follows

$$(1-\delta/\tau_k)\,A_k=B_k(-1/\tau_k)\equiv f_k^0/\tau_k \tag{44}$$

and by using (4) and (24) one can obtain

$$\hat{I}(0)=\sum_{k=1}^{n} f_k=\frac{\hat{I}_o(0)}{\hat{R}(0)}=\sum_{k=1}^{n}\frac{f_k^0}{1-\delta\tau_k^{-1}}. \tag{45}$$

Now, by using (41) and expanding $(1-\delta\tau_k^{-1})^{-1}$ to the first order in $\delta\tau_k^{-1}\ll 1$ it is possible to estimate δ from $Q(0)$ (given by (11)):

$$Q(0)+E_m(0)=\sum_{k=1}^{n} f_k^0[1+\delta\tau_k^{-1}+O(\delta^2\tau_k^{-2})],$$

$$\delta\approx\frac{Q(0)-\sum_{k=1}^{n} f_k^0}{\sum_{k=1}^{n} f_k^0\,\tau_k^{-1}}. \tag{46}$$

If $\delta\tau_k^{-1}$ is not small compared to one, the above expression is no longer valid. However, one can then numerically solve non-linear Eq. (45) for δ, where $\hat{I}(0)$ is again approximated by $Q(0)$. The fractions are then obtained from (44) and (4):

$$f_k=f_k^0/(1-\delta\tau_k^{-1}). \tag{47}$$

To calculate χ^2 when $\delta\neq 0$ we express C_i^R in terms of measured quantities (see (26–28)). The shift can always be written in the form $\delta=l\,h+\varepsilon$, $-h/2\leq\varepsilon\leq h/2$ where l is an

integer. Equation (39) can be now discretized to the first order in ε, so that (27) becomes

$$C_i^R = \int_{h(i-1)}^{hi} dt \int_0^t R(u+\delta)\, I^R(t-u)\, du$$
$$= \sum_{k=1}^{r} A_{kR} \left[\sum_{j=1}^{i-1} e^{h(i-j)/\tau_k^R} P_{jl} + P_{il}/2 \right] h + O(h^2/\tau_k^R), \quad (48)$$

$$P_{jl} = \tilde{R}_{j+l} + \varepsilon(\tilde{R}_{j+l+1} - \tilde{R}_{j+l})/h + O(\varepsilon^2). \quad (49)$$

Acknowledgements. We thank Dr. J. F. Hedstrom for providing a data for the preliminary phase of this study, and Dr. T. M. Therneau for helpful discussions on statistical issues. We also thank K. D. Peters for his assistance with preparation of the figures, and M. C. Stacy who was extremely efficient in keeping the computers and network running properly. It is our pleasure to acknowledge very valuable referee comments. Supported by grant GM 34847 of the USPHS.

References

Alcala JR, Gratton E, Prendergast FG (1987) Interpretation of fluorescence decays in proteins using continuous lifetime distributions. Biophys J 51:925–936

Ameloot M, Hendrickx H (1983) Extension for the performance of Laplace deconvolution in the analysis of fluorescence decay curves. Biophys J 44:27–38

Ameloot M, Beechem JM, Brand L (1986) Simultaneous analysis of multiple fluorescence decay curves by Laplace transforms. Deconvolution with reference or excitation profiles. Biophys Chem 23:155–171

Andre JC, Vincent LM, O'Connor D, Ware WR (1979) Applications of fast fourier transform to deconvolution in single photon counting. J Phys Chem 83:2285–2293

Aubard J, Levoir P, Denis A, Claverie P (1987) Direct analysis of chemical relaxation signals by a method based on the combination of Laplace transform and Padé approximants. Comput Chem 11:163–178

Bajzer Ž, Myers AC, Sedarous SS, Prendergast FG (1989a) Padé-Laplace method for the analysis of fluorescence intensity decay. Biophys J 56:79–93

Bajzer Ž, Myers AC, Sharp JC, Hedstrom JF, Prendergast FG (1989b) Padé-Laplace method for the analysis of time-resolved fluorescence decay curves. Biophys J 55:190a

Baker GA Jr (1965) The theory and application of Padé approximant method. Adv Theor Phys 11:58

Boens N, Malliaris A, Van der Auweraer M, Luo H, De Schryver FC (1988) Simultaneous analysis of single-photon timing data with a reference method: application to a Poisson distribution of decay rates. Chem Phys 121:199–209

Boens N, Janssens LD, De Schryver FC (1989) Simultaneous analysis of single-photon timing data for the one-step determination of activation energies, frequency factors and quenching rate constants. Application to tryptophan photophysics. Biophys Chem 33:77–90

Bronshtein IN, Semendyayev KA (1985) Handbook of mathematics. Van Nostrand, New York

Catterall R, Duddell DA (1983) Beyond chi-square: evaluation of parametric models used in the analysis of data from fluorescence decay experiments. NATO ASI (Adv Sci Inst) Ser A Life Sci 69:173–195

Demas JN, Adamson AW (1971) Evaluation of photoluminiscence lifetimes. J Phys Chem 75:2463–2466

Eisenfeld J (1983) Remarks on the method of moments for fluorescence decay analysis NATO ASI (Adv Sci Inst) Ser A Life Sci 69:223–231

Eisenfeld J, Ford CC (1979) A systems-theory approach to the analysis of multiexponential fluorescence decay. Biophys J 26:73–84

Gafni A (1983) Analysis of pulse fluorometry data by Laplace transforms NATO ASI (Adv Sci Inst) Ser A. Life Sci 69:259–270

Gafni A, Modlin RL, Brand L (1975) Analysis of fluorescence decay curves by means of the Laplace transformation Biophys J 15:263–280

Gauduchon P, Wahl P (1978) Pulse fluorimetry of tyrosil peptides Biophys Chem 8:87–104

Grinvald A, Steinberg IZ (1974) On the analysis of fluorescence decay kinetics by the method of least squares. Anal Biochem 59:583–598

Hall P, Selinger BK (1981) Better estimates of exponential decay parameters J Phys Chem 85:2941–2946

Hedstrom J, Sedarous SS, Prendergast FG (1988) Measurements of fluorescence lifetimes by use of a hybrid time-correlated and multifrequency phase fluorometer. Biochemistry 27:6203–6208

Isenberg I (1983) Robust estimation in pulse-fluorometry, a study of the method of moments and least squares. Biophys J 43:141–148

Isenberg I, Dyson RD (1969) The analysis of fluorescence decay by a method of moments. Biophys J 9:1337–1350

Jezequel JY, Bouchy M, Andre JC (1982) Estimation of fast fluorescence lifetimes with single photon counting apparatus and the phase plane method. Anal Chem 54:2199–2204

Kempthorn O, Folks L (1971) Probability statistics and data analysis Iowa State University Press, Ames, IA

Knutson JR, Beechem JM, Brand J (1983) Simultaneous analysis of multiple fluorescence decays curves: a global approach. Chem Phys Lett 102:501–507

Lanczos C (1956) Applied analysis. Prentice Hall, Englewood Cliffs, NJ

Libertini LJ, Small EW (1984) F/F deconvolution of fluorescence data. Anal Biochem 138:314–318

Livesey AK, Brochon JC (1987) Analyzing the distribution of decay constants in pulse-fluorometry using the maximum entropy method. Biophys J 52:693–706

Matheson (1989)The non-equivalence of Padé-Laplace and non-linear least squares data fitting: A Padé-Laplace bias towards slower processes. Comput Chem 13:385–386

McKinnon AE, Szabo AG, Miller DR (1977) The deconvolution of Photoluminiscence data. J Phys Chem 81:1564–1570

Mérola F, Rigler R, Holmgren A, Brochon JC (1989) Picosecond tryptophan fluorescence of thioredoxin: Evidence for discrete species in slow exchange. Biochemistry 28:3383–3398

O'Connor DV, Phillips D (1984) Time-correlated single photon counting, Academic Press, New York

O'Connor, DV, Ware WR, Andre JC (1979) The deconvolution of Photoluminiscence data. J Phys Chem 83:1333–1343

Press WH, Flannery BP, Tenkolsky SA, Vetterling WT (1986) Numerical recipes. Cambridge University Press, Cambridge

Scott TW, Campbell BF, Cone RL, Friedman JM (1989) Linear narrowing and site selectivity from proteins and glasses: cryogenic studies of conformational disorder and dynamics. Chem Phys 131:63–79

Sellinger BK, Harris CM (1983) A critical appraisal of analytical methods. NATO ASI (Adv Sci Inst) Ser A Life Sci 69:155–168

Small EW, Libertini LJ, Brown DW, Small JR (1989) Extensions of the method of moments for deconvolution of experimental data. RE (ed) Fluorescence detection III. In: Menzel, SPIE Proceedings 1054, Bellingham, Wash

Szabo AG, Bramal L (1983) Modulating functions – a deconvolution method. NATO ASI (Adv Sci Inst) Ser A Life Sci 69:271–283

Valeur B, Moirez J (1973) Analyse des courbes de décroissance multiexponentielles pa la méthode des fonctions modulatrices – application a la fluorescence. J Chim Phys 70:500–506

Vincent M, Brochon JC, Merola F, Jordi W, Gallay J (1988) Nanosecond dynamics of horse heart apocytochrome *c* in aqueous solution as studied by time-resolved fluorescence of the single tryptophan residue Trp-59. Biochemistry 27:8752–8761

Wijnaendts van Resandt RW, Vogel RH, Provencher SW (1982) Double beam fluorescence lifetime spectrometer with subnanosecond resolution: application to aqueos tryptophan. Rev Sci Instrum 53:1392–1397

Wild UP (1983) Fourier transform analysis. NATO ASI (Adv Sci Inst) Ser A Life Sci 69:239–257

Yeramian E (1986) Etude expérimentale et théorique de récepteurs de neuromédiateurs et déloppement de méthodologies pour l'analyse de signaux. PhD Thesis. Ecole Centrale des Arts et Manufactures

Yeramian E, Claverie P (1987) Analysis of multiexponential functions without hypothesis as to the number of components. Nature 326:169–174

Zucker M, Szabo AG, Bramal L, Krajcarski DT, Selinger B (1985) Delta function convolution method (DFCM) for fluorescence decay experiments. Rev Sci Instrum 56:14–22